

Cite this: *Phys. Chem. Chem. Phys.*, 2012, **14**, 5030–5044

www.rsc.org/pccp

PERSPECTIVE

Proton transfer and polarity changes in ionic liquid–water mixtures: a perspective on hydrogen bonds from *ab initio* molecular dynamics at the example of 1-ethyl-3-methylimidazolium acetate–water mixtures—Part 1†

Martin Brehm,^a Henry Weber,^a Alfonso S. Pensado,^a Annegret Stark^b and Barbara Kirchner*^a

Received 13th December 2011, Accepted 14th February 2012

DOI: 10.1039/c2cp23983c

The ionic liquid 1-ethyl-3-methylimidazolium acetate $[C_2C_1Im][OAc]$ shows a great potential to dissolve strongly hydrogen bonded materials, related with the presence of a strong hydrogen bond network in the pure liquid. A first step towards understanding the solvation process is characterising the hydrogen bonding ability of the ionic liquid. The description of hydrogen bonds in ionic liquids is a question under debate, given the complex nature of this media. The purpose of the present article is to rationalise not only the existence of hydrogen bonds in ionic liquids, but also to analyse their influence on the structure of the pure liquid and how the presence of water, an impurity inherent to ionic liquids, affects this type of interaction. We perform an extensive study using *ab initio* molecular dynamics on the structure of mixtures of the ionic liquid 1-ethyl-3-methylimidazolium acetate with water, at different water contents. Hydrogen bonds are present in the pure liquid, and the presence of water modifies and largely disturbs the hydrogen bond network of the ionic liquid, and also affects the formation of other impurities (carbenes) and the dipole moment of the ions. The use of *ab initio* molecular dynamics is the recommended tool to explore hydrogen bonding in ionic liquids, as an explicit electronic structure calculation is combined with the study of the condensed phase.

^a Wilhelm-Ostwald-Institut für Physikalische und Theoretische Chemie, Universität Leipzig, Linnéstr. 2, D-04103 Leipzig, Germany.
E-mail: bkirchner@uni-leipzig.de; Fax: +49 3419736399;
Tel: +49 3419736401

^b Institut für Technische Chemie, Universität Leipzig, Linnéstr. 3-4, D-04103 Leipzig, Germany

† Electronic supplementary information (ESI) available. See DOI: 10.1039/c2cp23983c

1 Introduction

During the last few years an important number of scientific articles have appeared in the literature concerning ionic liquids (ILs). They have been defined as new solvents, even if their history goes back more than one century,¹ as green solvents even if they can be quite toxic^{2–4} and non-volatile, even if some



Martin Brehm

Martin Brehm is currently a PhD student in the group of Barbara Kirchner at the University of Leipzig. Before taking this position, he studied chemistry in Leipzig. For creating his Bachelor thesis, he worked in the group of Mark Lautens in Toronto (Canada) for two months. Martin's work covers molecular dynamics and *ab initio* molecular dynamics, especially in the field of condensed phase molecular systems, as well as quantum chemical calculations of molecules.

Apart from that, he is the main developer of the program package TRAVIS, which is an open-source software for analyzing and visualizing molecular dynamics and Monte Carlo trajectories.



Henry Weber

Henry Weber is currently finishing his Master's Degree on Chemistry at the University of Leipzig. He worked as a student co-worker in the research group of Barbara Kirchner focusing mainly on structural and dynamical properties of ionic liquids. During this he was involved in a cooperative research project with the group of Hans-Peter Steinrück from the University of Erlangen-Nürnberg on the topic of anion–cation interaction in ionic liquids. After that he prepared his Bachelor

Thesis in the same research group, also at the University of Leipzig concerning molecular dynamics of ionic liquids.

experiments have probed that ILs can be distilled.^{5,6} The most accurate definition⁷ of ionic liquids could be: they are compounds constituted completely of ions, and their melting points are lower than 373 K. The anions and cations, usually voluminous,⁸ and characterized by molecular structures that are asymmetric and flexible with a delocalization of the electrostatic charges, can be independently selected to tune the IL's physicochemical properties (melting point, conductivity, viscosity, density, refractive index, *etc.*) while at the same time introducing specific features for a given application: hydrophobicity *vs.* hydrophilicity, controlling organic and inorganic solute solubility, adding functional groups for catalysis/reaction purposes,⁹ chirality,¹⁰ *etc.* Ionic liquids have a great potential in different applications, such as lithium batteries,^{11–13} dye-sensitized solar cells,^{14–17} lubricants,^{18,19} catalysis,^{20–22} to name a few.



Alfonso S. Pensado

ties. In January 2011 he accepted a postdoctoral research fellowship at the Theoretical Chemistry Group of the University of Leipzig. His research focuses on the use of computational tools to provide a best understanding of the physicochemical properties of new solvents, reaction media and technological fluids based on ionic liquids, with a high potentiality for a sustainable chemistry.



Annegret Stark

Friedrich-Schiller University of Jena, Germany (2003–2011) and habilitated before moving on to the University in Leipzig. Her main research interest is the application of ionic liquids to improve the sustainability of processes.

Annegret Stark has been working on ionic liquids since 1997, when she conducted her Honor's thesis research with Rob Singer (St. Mary's University Halifax, CA). After finishing her PhD with Ken Seddon (The Queen's University of Belfast, GB) she continued her career with a SASOL-sponsored post-doc scholarship with Halgard Raubenheimer (University of Stellenbosch, ZA). She established the Ionic Liquids research group at the

Although long-range Coulomb interactions are undoubtedly the strongest interactions amongst the forces between ions in the compounds,^{23–30} the importance of short-range dispersion interactions has recently become clear. These two types of interactions are responsible for the liquid structure of ionic liquids. The role of specific atomic features of the ions composing an ionic liquid leading to secondary structure-directing effects in the liquid phase is recognized as hydrogen bonding interactions.^{31–33} Goswami and Arunan³⁴ provided the more recent definition of a hydrogen bond, that is an extension of the previous one proposed by Pimentel and McClellan.³⁵ “A hydrogen bond is said to exist when: (1) there is evidence of a bond and (2) there is evidence that this bond specifically involves a hydrogen atom already bonded to another atom”.

Imidazolium based ionic liquids have in general high thermal stabilities, low melting points and low viscosities, when compared with ionic liquids composed of different cations.^{36–39} The evidence of the importance of hydrogen bonding in 1-alkyl-3-methylimidazolium ionic liquids was already highlighted by Seddon and coworkers⁴⁰ in 1986. Since then, the nature of hydrogen bonding in imidazolium based ionic liquids was intensely studied^{31,33,41–57} using a wide number of techniques, such as X-ray diffraction, mid-infrared and NMR spectroscopy, among others, as well as quantum chemistry calculations on systems containing a few ion pairs or classical molecular simulations.⁵⁸ The effect of the hydrogen bond on the physicochemical properties of ionic liquids is still being debated. The first evidence of the effect of eliminating the hydrogen bond ability of the imidazolium cation on the thermodynamic properties was provided by Bonhôte *et al.*,⁵⁹ when they observed that the methylation of the position C2 of 1-alkyl-3-methylimidazolium based ILs, and subsequently elimination of the C2-H2···X hydrogen bond leads to a liquid with higher viscosity and melting points, a somehow unexpected result (lower melting point and a decrease in viscosity would be expected³⁴). Huge efforts were made since then to rationalize the effect of hydrogen bonding on the physicochemical properties of imidazolium based ionic liquids. Thus, Hunt,⁶⁰ using different calculations (density functional theory methods, DFT) on ionic



Barbara Kirchner

in the condensed phase, to quantum chemical analysis of interesting molecules, and methodological developments. Barbara is also the editor of two Topics in Current Chemistry volumes and a series editor of Lecture Notes in Chemistry.

liquids based on the 1-butyl-3-methylimidazolium and 1-butyl-2,3-methylimidazolium cations, concluded that the effect of losing the hydrogen bonding is balanced by a decrease in entropy (the presence of a methyl group in the position C2 decreases the mobility of the anion, as was also stated by Zahn *et al.*²⁹), as the number of possible conformations that the anion can explore is much lower. The “entropy model” of Hunt assumes that hydrogen bonding stabilizes imidazolium based ionic liquids. A recent study of Endo *et al.*⁶¹ also supports the “entropy model”, as they conclude that the melting and freezing points of imidazolium based ionic liquids are increased with the methylation on position C2 of the imidazolium ring, due to an overcompensation of the phase transition entropy decrease for the enthalpy reduction. Ludwig’s group^{43,44,54,55} proposed a different approach to explain the relationship between molecular structure and macroscopical properties for imidazolium based ionic liquids. The authors suggest that the hydrogen bonds represent somehow “defects” on the Coulomb network of the ionic liquids, and their influence is towards fluidizing the ionic liquid, by increasing the dynamics of the cations and anions that leads to lower melting points and viscosities. They also show from the vibrational shifts towards higher wavenumbers in the far infrared (IR) and terahertz (THz) spectra that the interaction between cations and anions in imidazolium based ionic liquids is more intense due to the presence of hydrogen bonding. Hydrogen bonding leads to characteristic shifts in the NMR and IR spectra that reflect the changes in the chemical environment of the imidazolium cation.⁵⁶ Both the IR and the NMR spectroscopic properties reflect a similar type of electronic perturbation caused by the hydrogen bonding and the increase of the length of the C2–H bond. Noack *et al.*⁴⁸ studied the effect on the cation–anion interaction of including a methyl group in the position C2 of two different 1-alkyl-3-methylimidazolium cations, one with an ethyl side chain and the second one with a butyl side chain, linked with the bis(trifluoromethylsulfonyl)imide. Their spectroscopic work suggests that the electron density changes lead to changes in the position and strength of interionic interactions and reduced configurational variations, so a conjunction of both the “defect model” and the “entropy model” leads to a good description of the ionic liquid system. It is possible to conclude that hydrogen bonding is present in ionic liquids, and its presence affects the physicochemical properties of the ILs, and also that until now, no satisfactory theory or model can explain the effect of the hydrogen bonding on ionic liquids.

The ionic liquid 1-ethyl-3-methylimidazolium acetate, in the following referred to as $[C_2C_1Im][OAc]$, can be considered an enzyme-friendly co-solvent for biocatalysis,⁶² as well as a good solvent for strongly hydrogen bonding materials such as cellulose^{63–68} or chitin⁶⁹ and has significant ability to capture CO_2 .⁷⁰ The acetate anion is small and polar, capable to form hydrogen bonds with the 1-ethyl-3-methylimidazolium cation, as was identified by Dhumal *et al.*,⁴² using quantum chemistry calculations of an ion pair in the gas phase and spectroscopic techniques. These authors concluded that the lowest energy conformers exhibit strong C2–H \cdots O interionic interactions compared with other conformers. The carboxylate group (that is bidentate) is responsible for this strong directionality of the interactions. The interest of dissolving strongly hydrogen-bonding materials such as cellulose, lignin or chitin in ionic

liquids is to transform the raw material into useful products. The process involves a two-step procedure: first the raw material is mixed with the ionic liquid, usually at high temperature to decrease the viscosity of the mixture, and then, the addition of water solubilizes the IL, resulting in precipitation of the material. The potentiality of different ionic liquids to dissolve cellulose is related to their ability to form hydrogen bonds. Papanyan *et al.*⁵⁷ observed that the dissolution power of several ionic liquids based on the 1-ethyl-3-methylimidazolium cation, linked with the ethylsulfate and acetate anion can be correlated with shifts on the IR spectra, reflecting the interaction of the anion with the hydroxyl groups of cellulose. Thus, a good understanding of the hydrogen bonding in ionic liquids, and how the nature of these interactions depends on the type of anion is of great interest towards the development of new procedures to dissolve highly H-bonded materials.

Water is always present in ionic liquids, and can be considered as an impurity whose content can be minimized, but even in a “dry” ionic liquid some ppm of water are present. It is known for a long time that impurities influence many physicochemical properties of ILs.⁷¹ The ionic liquid 1-ethyl-3-methylimidazolium acetate is highly hygroscopic, so a comprehensive analysis on the effect of water on the structure of this IL will be very helpful towards understanding its behavior in different applications. The purpose of the present article is to provide insights into the intramolecular properties and the hydrogen bond network formed in the ionic liquid $[C_2C_1Im][OAc]$ and its mixtures with water as well as to comprehend the influence of the water concentration on the dipole moments of anions and cations and the polarizing/depolarizing effects of the ionic liquid towards the water molecules. A possible way to do that is using molecular simulation. There are several studies in the literature that consider the use of molecular simulation to understand the properties of mixtures of water and ionic liquids (see the excellent review of Klein and coworkers⁷²). Bowron *et al.*⁴¹ have explored the structure and dynamical properties of the ionic liquid $[C_2C_1Im][OAc]$ using neutron scattering and classical molecular simulation. This work was extended by the same group,⁵³ combining neutron diffraction, NMR and molecular dynamics to understand the solvation of glucose in this IL. Liu *et al.*⁷³ have performed an exhaustive study, by classical MD, to analyze the structure of binary and ternary mixtures of the ionic liquid 1-ethyl-3-methylimidazolium acetate with water and a cellulose oligomer.

To represent accurately the interactions present in the system ($[C_2C_1Im][OAc]$ –water), the use of methods such as density functional theory (DFT) or second-order Moller-Plesset perturbation theory (MP2), where the electronic structure of the molecules is explicitly considered, seems mandatory. The drawback of these techniques is that the calculations are usually performed with just a few molecules, being then not so representative of the liquid phase. On the other hand, classical molecular simulation, that is a well-known method to represent the structure and physicochemical properties of ionic liquids, which applies mostly pairwise additivity, is known to often lack the correct description of hydrogen bonding.^{74–77} We have considered *ab initio* molecular dynamics (AIMD), a method that combines an explicit electronic structure calculation using a DFT method with the sampling of a molecular dynamics

trajectory. Although AIMD methods are very reliable, they obey the “no free lunch theory”: one has to pay for reliable accuracy.

2 Computational details

To investigate the influence of the water amount on the properties of the system, we studied 4 different systems with different compositions, as shown in Table 1. The total amount of consumed CPU time for the simulations was more than 500 000 CPU hours (on AMD Opteron cores). The atom labeling⁷⁸ that will be used in this article as well as a snapshot of one of the simulation boxes (rendered with QuteMol⁷⁹) are presented in Fig. 1.

For each of the systems, a pre-equilibration was performed employing classical molecular dynamics within periodic boundary conditions, using the Gromacs program package⁸⁰ and the OPLS-AA force field⁸¹ with the additions from Liu *et al.*,⁸² who did a refinement of the force field for imidazolium-based ILs. 1 ns of physical time was simulated for each system, the simulation temperature was set to 350 K. A barostat was applied to adjust the pressure to 1 bar.

The starting configurations that resulted from this procedure were used to set up *ab initio* molecular dynamics simulations with the program package CP2k,⁸³ using the Quickstep module⁸⁴ and orbital transformation⁸⁵ for faster convergence. The electronic structure was calculated with density functional theory,^{86,87} utilizing the BLYP-D functional,^{88,89} which includes the empirical dispersion correction (D2) from Grimme.⁹⁰ Basis sets of the kind MOLOPT-DZVP-SR-GTH⁹¹ and GTH pseudopotentials^{92,93} were applied. The time step was chosen to be 0.5 fs. The temperature was set to 350 K by a Nose–Hoover chain thermostat.^{94–96} Each system was simulated for 10 ps with a barostat applied. The final box sizes were chosen to be the averages of the box sizes over the last 5 ps of these barostated runs. The resulting densities of the systems are given in Table 1. Subsequently, the production runs were performed, using a SCF convergence criterion of 10^{-5} . The physical simulation times shown in the table refer to the production runs. For the calculation of the dipole moments, maximally localized wannier centers (MLWCs)^{97,98} were computed in every 50th time step. For the pure ionic liquid, we find for the density a deviation of 0.9% with respect to the experimental value measured at 350 K. The density of $[\text{C}_2\text{C}_1\text{Im}][\text{OAc}]$ (Iolitec, Lot G001101.4) has been determined using a sand bath ($T = \pm 0.2$ K) in a BYK midget density cup (density values as a function of the temperature are presented in Table 2).

Table 1 The 4 investigated systems (IP refers to ion pairs of $[\text{C}_2\text{C}_1\text{Im}][\text{OAc}]$)

System	A	B	C	D
Composition	36 IP	27 IP	3 IP	
		81 H_2O	300 H_2O	128 H_2O
Percentage m/m	100	75.9	8.6	0
	0	24.1	91.4	100
x_{water}	0	0.75	0.99	1
Density/g cm^{-3}	1.066	1.000	1.001	0.996
Box size/pm	2121	2158	2141	1567
Physical time/ps	47.2	61.6	49.0	53.9
CPU hours	138 800	149 333	122 267	33 460

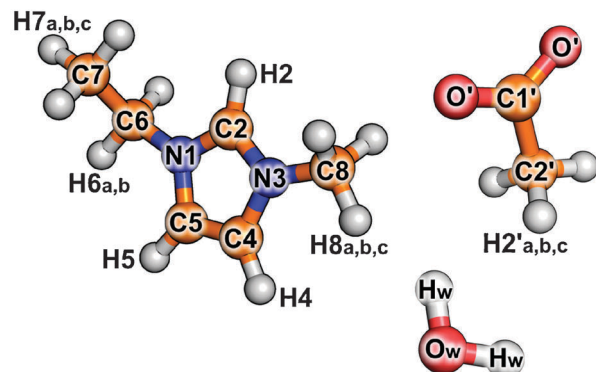


Fig. 1 The atom labeling⁷⁸ used throughout this article (upper panel); a snapshot⁷⁹ of one of our simulation boxes (lower panel).

The analysis of the trajectories was performed with TRAVIS, our recently published free software.⁹⁹ Details on the performed analyses can be found in the article about TRAVIS. The 2D diagrams were created using XmGrace.¹⁰⁰ For the 3D contour plots, Wolfram Mathematica¹⁰¹ was used.

3 Results and discussion

We will identify along the manuscript the four studied systems with the labeling scheme presented in Table 1. We will use the following coloring scheme: black curves depict system A, red curves system B, blue curves system C, and green curves system D.

3.1 Density

The liquid density data for the pure ionic liquid 1-ethyl-3-methylimidazolium acetate measured as a function of the temperature are provided in Table 2. The uncertainty in the measurement was ± 0.003 g cm^{-3} . The data were well correlated using linear regression as a function of temperature, as shown in Fig. S1 of the ESI†: $\rho(T) = 1.2584 - 5.205 \times 10^{-4} T$ (with ρ in g cm^{-3} and T in K). The average absolute deviation between our present density data of $[\text{C}_2\text{C}_1\text{Im}][\text{OAc}]$ and those reported by Shiflett and Yokozeki⁷⁰ is 0.3%.

Table 2 Experimental density data for $[C_2C_1Im][OAc]$

T/K	$\rho/g\ cm^{-3}$
292.15	1.106
300.40	1.102
310.75	1.097
321.15	1.091
330.50	1.087
340.95	1.081
350.70	1.076
357.15	1.072

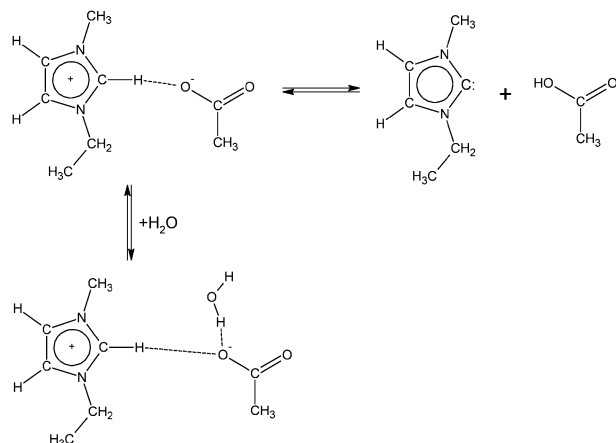
3.2 Intramolecular properties

To study the effect of the local environment on the molecules, we performed statistical analyses on characteristic bond lengths and angles of the cation and anion. The results are given in Table 3. The information gathered from the bulk phase simulations is compared with the values obtained from geometry optimisation of single molecules under vacuum (using the same computational method for the electronic structure).

The length of the bond C2–H2 in $[C_2C_1Im]^+$ decreases when water is added to the system. The mean value changes only slightly, but the maximum value of the bond length reached decreases drastically (from over 130 pm in the pure IL to 121.7 pm in the very dilute system: the distribution is presented in Fig. S2 of the ESI†). In the pure IL, very strong forces act upon the atom H2 and the bond is almost broken in some situations (see Section 3.4). This effect can only be observed in the pure IL and almost vanishes when a certain amount of water is added. This fact was also observed by Wulf *et al.*⁵⁶ using IR and NMR spectroscopy. In all three simulated systems, the C2–H2 bond is longer than for a single molecule under vacuum, in accordance with the observed formation of carbenes in this ionic liquid, both using experimental techniques¹⁰² and quantum chemistry calculations¹⁰³ on a single ion pair (see the scheme presented in Fig. 2). A similar trend as seen for H2, but less distinct, is observed for the other two hydrogen atoms, H4 and H5, at the rear of the imidazolium ring (see ESI†), as they are less protic and therefore they interact weakly with the acetate anion.

Table 3 Statistical data on bond lengths/angles in the simulated molecules. “Mono” refers to an isolated monomer calculation of the specified molecule in vacuum at 0 K. σ is the standard deviation

System	Bond/angle	Mean	σ	Min	Max
A	$[C_2C_1Im]^+$ C2–H2	109.7 pm	3.4	97.0	130.7
B		109.0 pm	3.1	96.1	126.9
C		108.7 pm	3.2	97.8	121.7
Mono		108.19 pm			
A	$[OAc]^-$ C1'–C2'	155.4 pm	4.0	140.0	179.7
B		154.4 pm	4.0	139.1	175.6
C		153.2 pm	3.7	140.4	169.0
Mono		158.42 pm			
A	$[OAc]^-$ C1'–O'	128.2 pm	2.6	116.5	143.8
B		128.5 pm	2.7	116.8	144.3
C		128.7 pm	2.7	118.1	140.5
Mono		127.27 pm			
A	$[OAc]^-$ O'–C1'–O'	125.5°	3.0	112.3	138.8
B		124.3°	3.0	111.6	137.9
C		123.1°	3.0	111.0	135.2
Mono		129.52°			

**Fig. 2** Proposed paths for the formation of carbenes and acetic acid in the $[C_2C_1Im][OAc]$ ionic liquid in the presence of water.

The C1'–C2' bond in $[OAc]^-$ is also reduced in its length when the amount of water increases. The bond length of one acetate molecule under vacuum is significantly larger than the mean values observed in the simulations of the bulk phase, a fact that also is observed for the C1'–O' bond length (see ESI†). The value of the angle O'–C1'–O' in $[OAc]^-$ is reduced when the water content increases. The angle observed in the pure IL is significantly smaller than the angle observed for one molecule under vacuum. The presence of ionic liquid has no effect on the bond length and angle of water.

3.3 Radial distribution functions

The radial distribution functions (RDFs) between several representative atoms of $[OAc]^-$ and $[C_2C_1Im]^+$ are given in Fig. 3. Panel (a) presents the RDFs between the three hydrogen atoms of the imidazolium ring (H2, H4 and H5) and the oxygen atoms O' of the $[OAc]^-$ for the pure ionic liquid. From the maximum of the curve, which is found at around 200 pm, it can be seen that the coordination of the anion to the atom H2 is much more distinct and also somewhat tighter than for the other two atoms, suggesting that H2 is a stronger hydrogen bond donor than H4 and H5. The coordination of $[OAc]^-$ to H4 and H5 is almost identical, suggesting that the side chain has only small influence on the (structural) coordinating behavior. These findings are in agreement with previous AIMD studies^{104,105} on imidazolium based ionic liquids, where a pronounced coordination of the anion towards the most acidic hydrogen atom of the imidazolium ring was observed as well.

We compare in panel (b) of Fig. 3 the radial distribution functions between the hydrogen atom H2 of the cation and the oxygen atoms of the anion and water for the 3 systems. The first peak is much higher for the pure IL than for system B and the average distance of the first coordination shell is shifted slightly outwards when water is added. Also shown in the plot is the coordination of water to H2 (given by the dashed lines). Water molecules compete with $[OAc]^-$ anions to be placed close to H2, but the anion coordinates stronger than water, as the peak of the RDF is higher in the case of the anion (see the red curves of panel (b) in Fig. 3). Interestingly, with further increase of the water content (system C) the coordination of

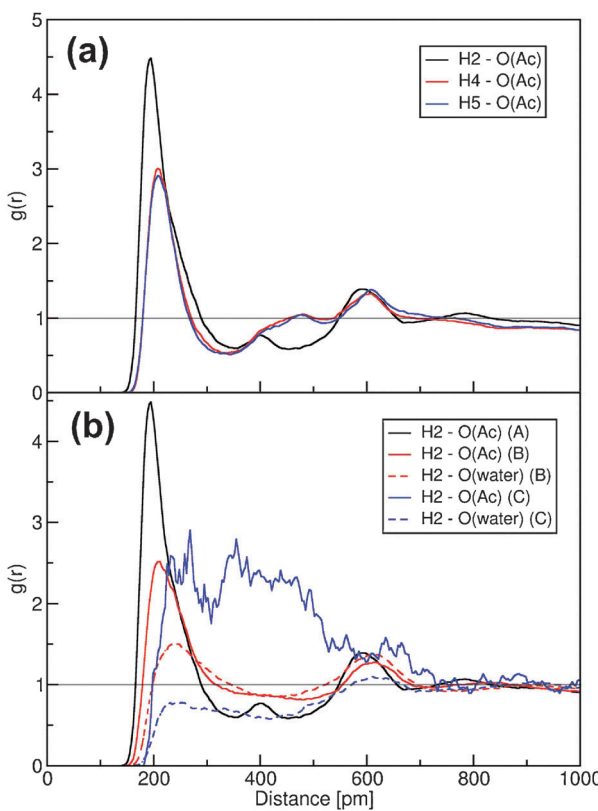


Fig. 3 Cation–anion and cation–water site-site radial distribution functions (RDFs): (a) oxygen atoms of the $[\text{OAc}]^-$ anion around the hydrogen atoms of the imidazolium ring of the $[\text{C}_2\text{C}_1\text{Im}]^+$ cation (system A); (b) solid lines: hydrogen atom H2 of the $[\text{C}_2\text{C}_1\text{Im}]^+$ around the oxygen atoms of the $[\text{OAc}]^-$ anion, dashed lines: hydrogen atom H2 of the $[\text{C}_2\text{C}_1\text{Im}]^+$ around the oxygen atoms of water.

water to H2 is lowered, indicating that H2 is not a strong hydrogen bond donor with respect to water. This result is in accordance with the observations made by several research groups:^{106–109} Mele and coworkers^{106,108} observed that for small water contents, the interaction of water is specific and localized at H2, H4, and H5 protons, those capable of establishing hydrogen bonds with water. At higher water content the interaction of water with the other protons of the side chains increases considerably and does not show any preference, and Welton and coworkers¹⁰⁷ also observed that the cation has a minor effect on the coordination of water when compared with the anion. The peak present in the RDFs of Fig. 3 at distances around 600 pm for systems A and B is related to the $[\text{OAc}]^-$ and water molecules coordinating to the back side of the imidazolium ring (H4 and H5).

The same analysis was also performed for the other two ring hydrogen atoms H4 and H5 (see Fig. S3 and S4 of the ESI†). In contrast to the coordination to H2, water is here a stronger competitor to $[\text{OAc}]^-$. This is reflected in the same coordination of water and $[\text{OAc}]^-$ to H4 and H5 in system B, as opposed to the behavior of H2. As observed for H2 with even higher water concentration (system C) the coordination of water at H4 and H5 is lowered. Probably due to the closer proximity of H4 to the ethyl side chain than to the methyl group, the coordination of the $[\text{OAc}]^-$ anion at H4 is much

stronger than at H5. This effect will be further investigated in part 2 of our article.

We analyze now the influence of the ionic liquid on the structure of water. Fig. 4 presents the radial distribution functions between a given hydrogen atom of a water molecule and the oxygen atom of a second water molecule or an acetate anion (panel (a)). Panel (b) depicts the RDFs between the oxygen atom of a water molecule and the different hydrogen atoms of the imidazolium ring of the $[\text{C}_2\text{C}_1\text{Im}]^+$ cation, in comparison with the equivalent oxygen–hydrogen RDF of water molecules.

The radial distribution functions between Ow and Hw show that the water gets more structured when the ionic liquid content increases, reflected by an increase in the height of the first (and second) peak of the RDF (see Fig. 4). The effect is more marked for system B. These findings are in good agreement with previous AIMD studies, as that performed by Spickermann *et al.*¹¹⁰ for the mixture of the ionic liquid 1-ethyl-3-methylimidazolium chloride–water. The width of the first solvation shell (defined by the position of the first minimum) is somewhat increased when more IL is added, indicating that the hydrogen bonds between water molecules are longer than in neat water. This was rather unexpected, because a higher structuring and therefore a stronger

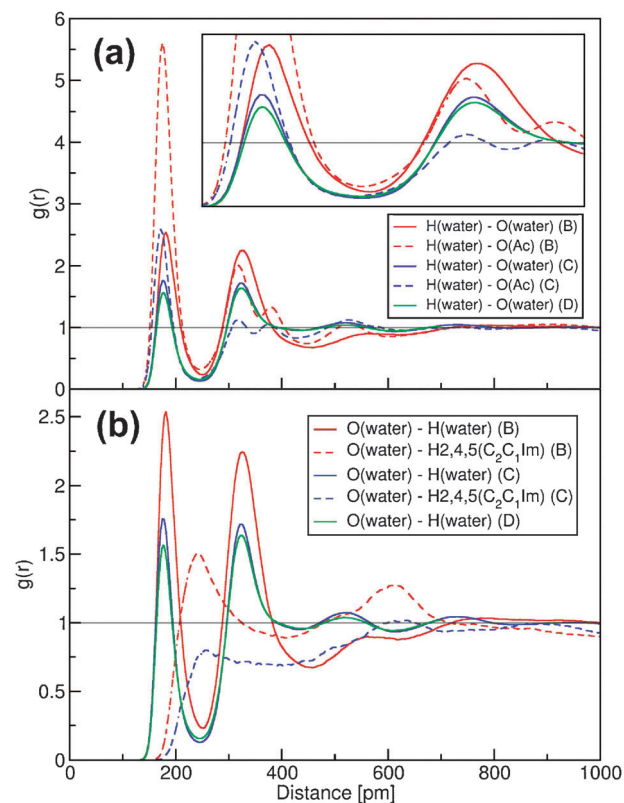


Fig. 4 Changes in the water structure: (a) solid lines: RDF between the hydrogen atom Hw of a water molecule and the oxygen atom Ow of a second water molecule, dashed lines: RDF between the hydrogen atom Hw of a water molecule and the oxygen atom O' of a $[\text{OAc}]^-$ anion; (b) solid lines: RDF between the hydrogen atom Hw of a water molecule and the oxygen atom Ow of a second water molecule, dashed lines: RDF between the hydrogen atoms of the imidazolium ring of a $[\text{C}_2\text{C}_1\text{Im}]^+$ cation and the oxygen atom Ow of a water molecule.

interaction usually corresponds to a decrease of the hydrogen bond length.¹¹⁰

The dashed lines in panel (a) of Fig. 4 show that the interaction between water and acetate is very strong, as it can be seen from the large first maximum for systems B and C, in both cases significantly larger than the maximum of the water Ow–Hw RDF. The distance of the water–acetate maximum is found to be around the same distance as the water Ow–Hw maximum. A different behavior of the cations is apparent from the dashed lines in panel (b) of Fig. 4, which reflect the interaction between the hydrogen atoms H2, H4 and H5 of the $[C_2C_1\text{Im}]^+$ cation and the oxygen atom of water. For system B, we find a high peak, however smaller than the water Ow–Hw maximum. In system C, there is almost no coordination of water to the hydrogen atoms of the ring of the cation. Both for systems B and C, the coordination distance is strongly increased in comparison to the position of the first maximum on the Ow–Hw RDF, indicating the presence of weak interactions between $[C_2C_1\text{Im}]^+$ and water.

Fig. 5 presents the Ow–Ow and the Hw–Hw RDFs for water. A similar trend is observed for these functions: with increasing ionic liquid content, the water gets more structured, reflected by higher peaks in the RDF. Panel (b) shows that, for the Ow–Ow interaction in system B, only the first maximum is stronger, whereas the second maximum almost vanishes. This is due to the relatively low water content of system B (“low” in regard to the mass fraction, not the mole fraction). No bulk water network can

be formed there, and the water is found in small but strongly bound “isles”, which is an indication for microheterogeneity in system B.

3.4 Proton transfer and carbene formation

We presented in Section 3.2 the distribution of the bond lengths between the carbon atom C2 and the hydrogen atom H2 of the imidazolium ring of the $[C_2C_1\text{Im}]^+$, observing that the mean value of the length of this particular bond does not differ significantly from the value obtained for an isolated cation, but strong fluctuations occur. A distance as long as 130 pm was observed during the simulation. This can lead to the assumption that there are configurations where the C2–H2 bond is almost broken. A comprehensive analysis of the bond lengths is performed to evaluate the possibility of carbene formation, this process is summarized in the diagram presented in Fig. 2.

Fig. 6 shows a combined distribution function where the X axis corresponds to the C2–H2 bond length of the $[C_2C_1\text{Im}]^+$ cation and the Y axis depicts the distance between the atom H2 of the cation and an oxygen atom of the closest $[\text{OAc}]^-$ anion. In the case of the pure ionic liquid, when an oxygen atom of the anion is placed at a distance larger than 200 pm from the hydrogen atom H2 of the cation, the distribution of the C2–H2 bond length is almost symmetrical and centered in the equilibrium distance (100–120 pm). When the distance between O' and H2 is shorter, we observe an increase in the C2–H2 bond length. The oxygen atoms of $[\text{OAc}]^-$ attract the acidic hydrogen atom H2 so much that it is almost being abstracted, because acetic acid is a weak acid,¹⁰³ causing an elongation of the C2–H2 bond. The red lines in Fig. 6 indicate when the hydrogen atom H2 is at the same distance to the carbon atom C2 as one of the oxygen atoms O' of the acetate anion. For system A, the criterion for the hydrogen atom H2 being shared between C2 and O' is fulfilled

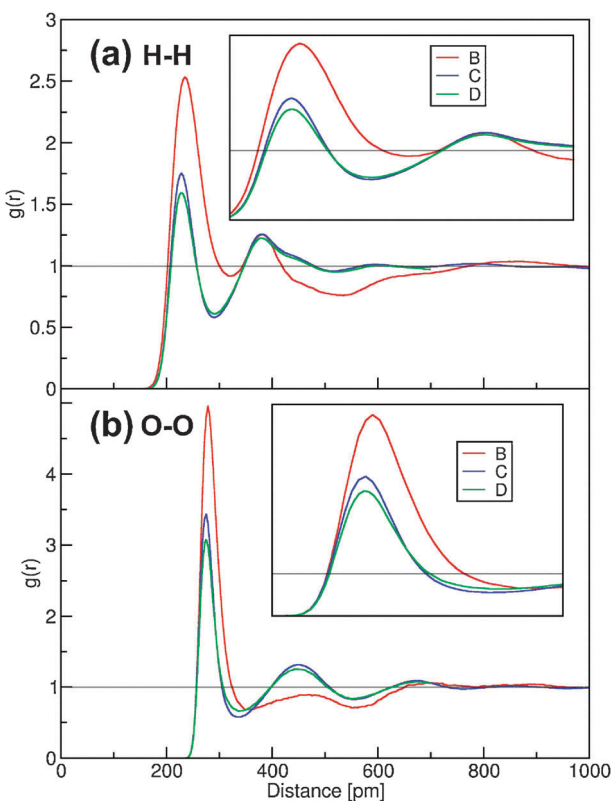


Fig. 5 Changes in the water structure: (a) RDF between the hydrogen atoms Hw of a water molecule and the hydrogen atoms Hw of a second water molecule, (b) RDF between the oxygen atom Ow of a water molecule and the oxygen atom Ow of a second water molecule.

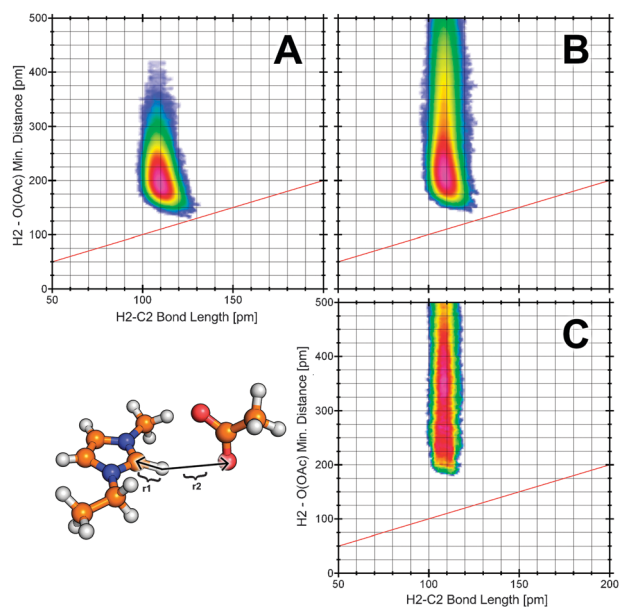


Fig. 6 Combined distribution function showing the abstraction of the $[C_2C_1\text{Im}]^+$ H2 atom by $[\text{OAc}]^-$. The red line indicates configurations where $r_1 = r_2$.

for some conformations during the length of the simulation. There are cases where the C2–H2 bond is virtually broken (which is possible in AIMD simulations) and the proton is (almost) abstracted. Regarding that imidazolium-based ILs are usually classified as aprotic ILs, the present result is quite interesting, as it shows clearly the strength of the hydrogen bond between $[\text{OAc}]^-$ and $[\text{C}_2\text{C}_1\text{Im}]^+$, and therefore they should not be considered anymore in the general case as aprotic.¹⁰³ The addition of water to the ionic liquid makes the possible proton abstraction less probable (see Fig. 6) as the distances between the H2 and O' are larger. Our results agree with recent experimental studies, showing that in the $[\text{C}_2\text{C}_1\text{Im}][\text{OAc}]$ ionic liquid the abstraction of the H2 atom by the $[\text{OAc}]^-$ may occur, leading to the formation of carbenes.¹⁰² Our findings indicate that the carbene formation will only take place if the IL is dry, and the successive addition of water will minimize this effect. This can also be achieved by tuning of the basicity of the anion.^{56,57,103} Carbenes presented in pure $[\text{C}_2\text{C}_1\text{Im}][\text{OAc}]$ can be considered as an intrinsic impurity (even able to act as a catalyst¹¹¹ in benzoin condensation, hydroacylation and also in oxidation of an alcohol by using CO_2w and air) that cannot be eliminated from the IL, so for the use of this particular IL in different applications, this aspect (impurities) should not be disregarded. The formation of carbenes is more favourable at low pressures,¹⁰³ whereas in the bulk phase the equilibrium is shifted towards the stability of the ion pairs, so the extraction of different compounds dissolved in the ionic liquid by applying vacuum conditions can lead to the degradation of the ionic liquid.

We also investigated the coordination of water molecules to the hydrogen atom H2 of the $[\text{C}_2\text{C}_1\text{Im}]^+$ cation, and the effect on the C2–H2 bond elongation.¹¹² The corresponding CDFs (equivalent to Fig. 6) are presented in Fig. S5 of the ESI.[†] There are no configurations where the C2–H2 bond length is similar to the corresponding H2–Ow (water) distance. The water molecules are not pulling on the H2 atom, and therefore water does not lead to carbene formation. The different behavior observed for water and $[\text{OAc}]^-$ leads us to conclude that the hydrogen bond formed between H2 and O' ($[\text{OAc}]^-$) is substantially stronger than that formed between H2 and Ow (water), independently of the IL/water mixing ratio. The proton abstraction from the point of view of thermodynamics is well characterized by the pK_a values. Regarding the much higher pK_a value of 24 for H2 in the *N,N'*-diisopropyl-4,5-dimethylimidazolium cation¹¹³ and 23 for the 1,3-dimethylimidazolium cation¹¹⁴ in contrast with the pK_a value of 7 for water, it is not surprising that the bond elongation is much more distinct when $[\text{OAc}]^-$ is coordinating to $[\text{C}_2\text{C}_1\text{Im}]^+$ H2 rather than water.

The acetate anion forms very strong hydrogen bonds with water that can lead to the abstraction of a proton from the water molecule. Fig. 7 presents a CDF with the length of the Ow–Hw bond on the X axis, and the distance between the hydrogen atom of water and the closest oxygen atom of an $[\text{OAc}]^-$ anion on the Y axis. Events under the red line indicate that the distance of the hydrogen atom of water to the acetate is shorter than the bond length. When the acetate anion is placed close to the water molecules, there are conformations where one hydrogen atom of the water molecule is shared with

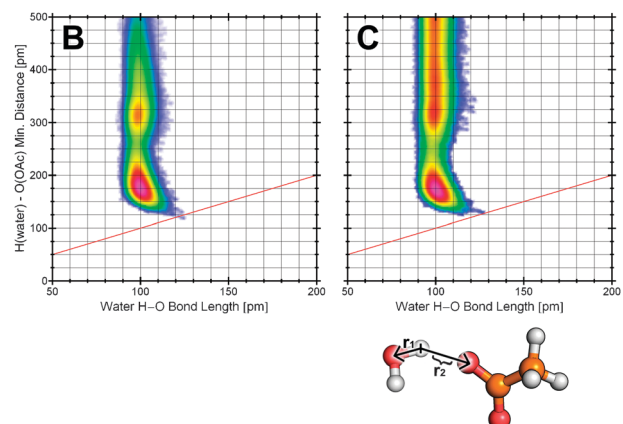


Fig. 7 Combined distribution function showing the abstraction of a water H atom by $[\text{OAc}]^-$. The red line indicates configurations where $r_1 = r_2$.

the anion, leading to the formation of acetic acid. The increase of water content in the system has an insignificant effect on the proton abstraction. A similar analysis is carried out for water, Fig. 8 presents a CDF in which the X axis presents the bond length Ow–Hw of water and the Y axis the distance of the given hydrogen of water to the closest oxygen atom of a second water molecule, where the red line indicates when an hydrogen atom is “shared” between two water molecules. In pure water (system D) it is possible to find some conformations where the hydrogen bond has the same length as the covalent bond, a well known fact that leads to the autodissociation of water. The high energy barriers avoid observation of this phenomenon in *ab initio* molecular dynamics simulations without the use of specific techniques to sample rare events, nevertheless, our results indicate that the bond dissociation occurs in pure water at moderate temperatures. The addition of small quantities

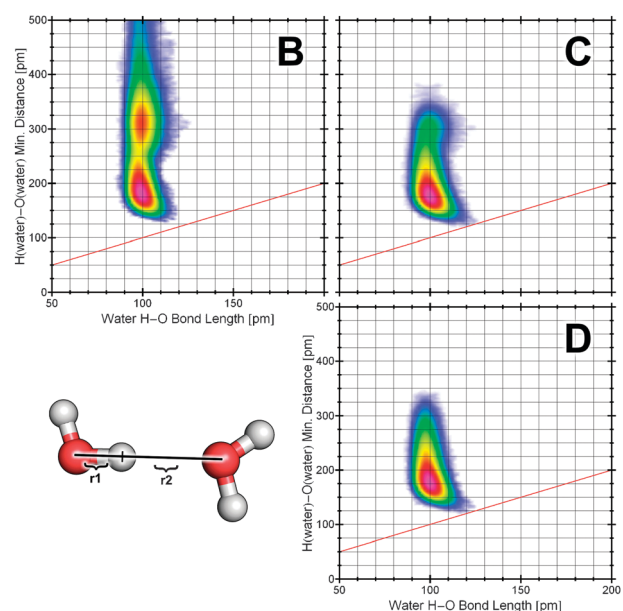


Fig. 8 Combined distribution function showing the abstraction of an H atom from water by another water molecule. The red line indicates configurations where $r_1 = r_2$.

of ionic liquid to water does not change the behavior observed for pure water, but when the quantity of ionic liquid is larger (as is the case of system B), the minimum distance between hydrogen atoms of a water molecule and the oxygen of a second water molecule increases, leading to a lower probability of water dissociation. It is possible to conclude from our results that in the ionic liquid $[C_2C_1Im][OAc]$ (which will always have some water content) a given number of impurities will be present that are inherent at the particular nature of this ionic liquid. This fact should be taken into account when selecting this particular IL for a given application.

3.5 Dipole moments

Wendler *et al.*¹¹⁵ have calculated the dipole moments of the ionic liquids 1-3-dimethylimidazolium chloride $[C_1C_1Im][Cl]$, 1-ethyl-3-methylimidazolium thiocyanate $[C_2C_1Im][SCN]$ and 1-ethyl-3-methylimidazolium dicyanoamide $[C_2C_1Im][DCA]$ from AIMD simulations. The authors found that the range of dipole moments is broad due to fluctuations, and that the electrostatic interactions are quite local due to screening of the ion charges, a result previously stated by Lynden-Bell.¹¹⁶ We have used the same methodology as Wendler *et al.*¹¹⁵ to obtain the dipole moments of the $[C_2C_1Im]^+$ cation, $[OAc]^-$ anion and water, for the four systems considered in this work.

For a system of particles with a total neutral charge, the dipole moment is uniquely defined. The same does not hold true for charged particle distributions, where a reference point needs to be chosen that will influence the obtained values of the dipole moment. There is no *best choice* of this reference point. One possible choice is taking the center of mass as the reference point but this option suffers from “isotope effect”, *i.e.* if one of the atoms is replaced by a different isotope, the center of mass moves and therefore the calculated dipole moment is different, whereas the electronic structure remains unaltered so the dipole moment will not change. Another possibility is taking the center of geometry of the ion, but for the particular case of alkylimidazolium cations, this choice can lead to illogical results, *i.e.*, if a long alkyl (non-polar) chain is attached to the imidazolium ring, the center of geometry will be shifted, whereas the dipole moment will remain almost unaltered. Therefore, for imidazolium cations, we suggest the use of the geometrical center of the ring as the reference point. The dipole moments calculated according to this reference point are the same if one atom is substituted by a different isotope, and the inclusion of long non-polar side chains will not modify substantially the dipole moment. Summarizing, we have considered for the $[C_2C_1Im]^+$ cation the geometric center of the five ring atoms (CoR) as the reference point, whereas for the $[OAc]^-$ the center of geometry (CoG) is taken into account, the same criteria as used by Wendler *et al.*¹¹⁵ in their work. The dipole moments of the cation, anion and water are listed in Table 4. The effect of the considered reference point (the center of geometry (CoG), center of mass (CoM)) on the values of the dipole moment of the cation is presented in the ESI.† Fig. 9 shows the different distribution of the dipole moment of the cation considering the three reference points (center of geometry, CoG; center of mass, CoM; and geometrical ring center, CoR). Large changes

Table 4 Statistical data on the dipole moments of the simulated molecules. Ref. indicates the reference center for dipole calculation of charged particles: CoG = center of geometry, CoR = geometric center of ring. All values are in Debye

System	Molecule	Ref.	Mean	σ	Min	Max
A	$[C_2C_1Im]^+$	CoR	2.84	0.67	0.26	5.11
B			2.87	0.62	0.62	5.11
C			2.80	0.55	1.01	4.60
Mono			2.37			
A	$[OAc]^-$	CoG	8.84	0.45	7.36	10.91
B			9.28	0.48	7.17	11.31
C			10.04	0.51	8.42	11.81
Mono			6.68			
B	H_2O		2.80	0.31	1.77	4.35
C			3.04	0.30	1.53	4.90
D			3.00	0.30	1.78	4.80
Mono			1.83			

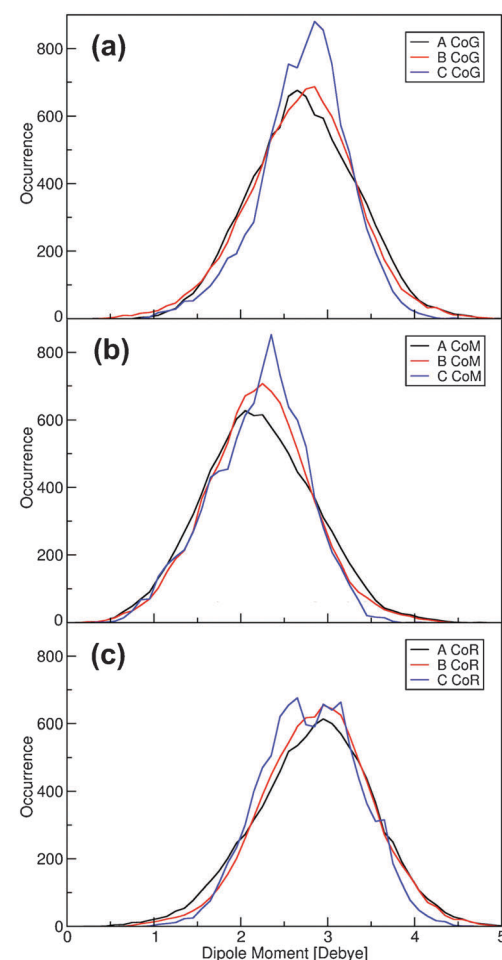


Fig. 9 Dipole moment distribution functions for the $[C_2C_1Im]^+$ cation in three different systems, using 3 different reference centers for dipole calculation: (a) CoG = center of geometry, (b) CoM = center of mass, (c) CoR = geometric center of ring.

in the mean values are observed for the different reference points, whereas the width of the distributions remains mainly unaffected.

As shown in Table 4, the mean value of the dipole moment of the $[C_2C_1Im]^+$ cation remains constant when the water content increases. For all three bulk systems (systems A, B and C), the

cation possesses a larger dipole moment than under vacuum. For the $[OAc]^-$ anion, the observed trend is different: the dipole moment is strongly increased with the amount of water, and all bulk-phase systems show a larger dipole moment for $[OAc]^-$ than the vacuum calculation. The dipole moment of the anion in a bulk phase comes close to the value obtained in the gas phase when the concentration of water decreases (see Fig. 10). This result agrees with the fact that acetate is a very strong hydrogen bond acceptor and tightly incorporates into the hydrogen bond network of the water. The $[C_2C_1Im]^+$ cation is only a weak hydrogen bond donor and therefore shows almost no interaction with water molecules (reflected by the similar values of the dipole moment when the water content increases). The dipole moment of water decreases with increasing amount of ionic liquid (see Table 4): the water gets depolarized by the IL. This was also reported by Spickermann *et al.*¹¹⁰ for the mixture 1-ethyl-3-methylimidazolium chloride–water as well as Zahn *et al.*¹¹⁷ for the mixture mono-methylammonium nitrate–water. However, the dipole moment of water is still substantially larger than the value of one isolated water molecule under vacuum, a fact related to the strong cooperativity of water: strong hydrogen bond network.

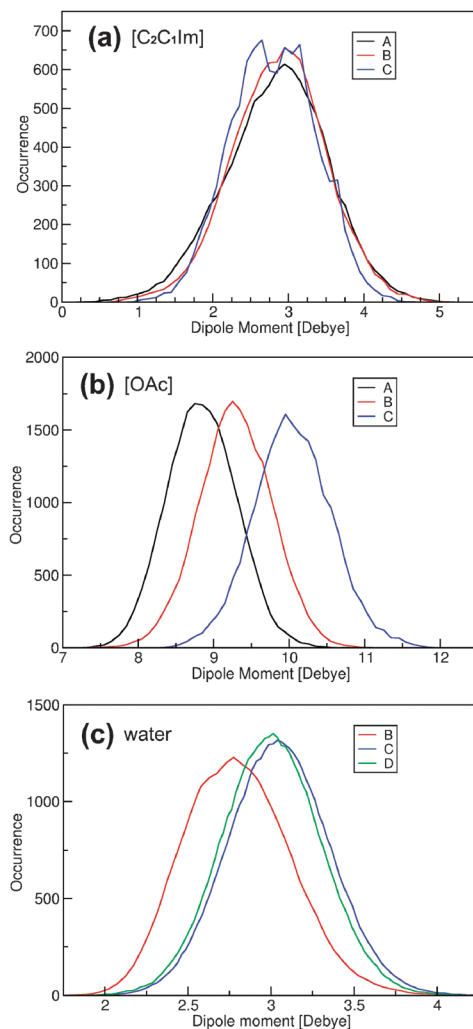


Fig. 10 Dipole moment distribution functions: (a) dipole moment of $[C_2C_1Im]^+$ (CoR); (b) dipole moment of $[OAc]^-$ (CoG); (c) dipole moment of H_2O .

This effect was already observed by several authors, Silvestrelli and Parrinello¹¹⁸ for pure water, or Kirchner and Hutter¹¹⁹ for a DMSO–water mixture. The dipole moment of the water molecules in the bulk phase^{118,119} is significantly larger than for isolated water molecules under vacuum. The trends of the dipole moment for the cation, anion and water for the different systems considered in this work are summarized in Fig. 10.

To gain insight into the effect of the anions and cations on the dipole moment of water molecules, we calculate the dipole moments of water molecules that are first neighbors (defined over the distance between the centers of mass) to the $[C_2C_1Im]^+$ cations and $[OAc]^-$ anions. The resulting histograms are shown in Fig. 11. The water molecules possess different dipole moments depending on their local environment. Water molecules located in proximity to a $[C_2C_1Im]^+$ cation in system B present in average the same value of the dipole moment as the ensemble of all the water molecules in the system (but lower than in pure water). When the content of ionic liquid decreases, water molecules in proximity of the cations present lower values of the dipole moment than the average value over all the systems (see panel (a) of Fig. 11). We can conclude that the cation exhibits a depolarizing effect on water, and this effect is stronger when the concentration of ionic liquid increases. Water molecules directly adjacent to $[OAc]^-$ anions are strongly polarized, and the strength of this polarization is similar in systems B and C (around 0.2 Debye). Even if the effect of the anion is to polarize the water molecules, in the system with high ionic liquid content, the average value of the dipole moment of water is decreased (when compared with pure water).

In order to elucidate the effect of the local environment on the dipole moment of water, it is possible to construct a combined distribution function, where the dipole moment of a molecule can be represented as a function of a certain

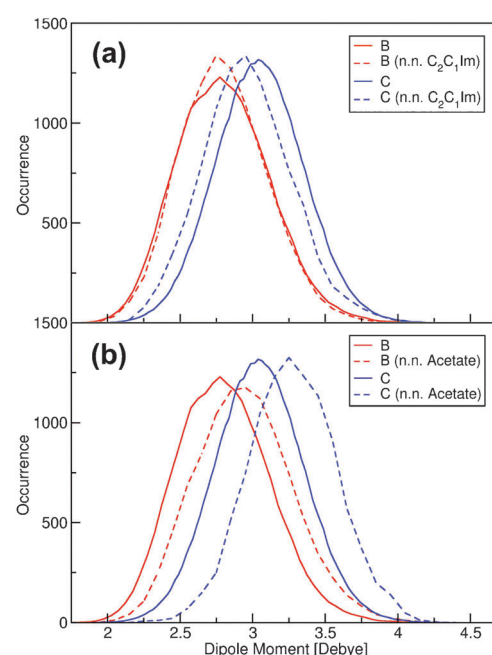


Fig. 11 Dipole moment distribution functions for water molecules which are next neighbors (n.n.) of (a) $[C_2C_1Im]^+$ and (b) $[OAc]^-$ ions in comparison to the water molecule average (solid lines).

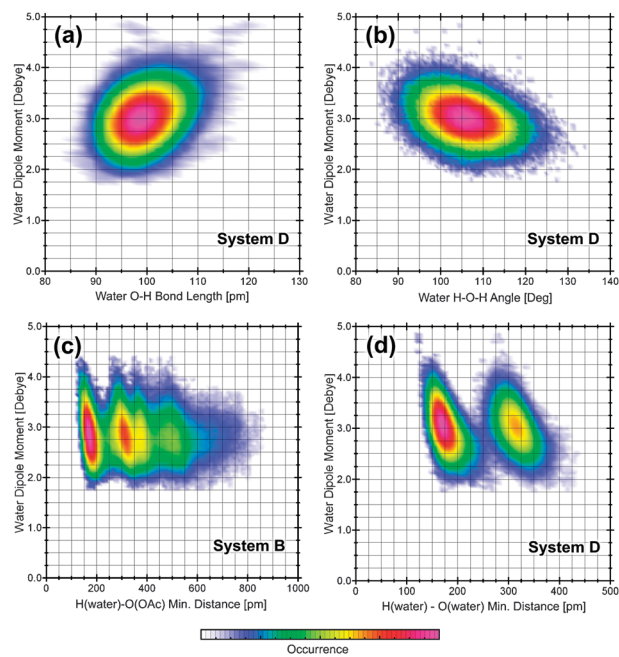


Fig. 12 Dependence of the water dipole moment on the Ow–Hw bond length (a) and Hw–Ow–Hw angle (b) for system D; dependence on distance to the oxygen atoms of the nearest $[OAc]^-$ anion (c) for system B; dependence on length of the donated hydrogen bond (d) for system D.

distance or angle. Four different plots are given in Fig. 12. Panels (a) and (b) present the dependence of the dipole moment of a water molecule on the Ow–Hw bond length and Hw–Ow–Hw angle of that molecule for system D. Higher dipole moments are obtained when the bond length increases or the Hw–Ow–Hw angle decreases, a result that can be explained with a simple picture of 3 point charges: the more they separate, the stronger the dipole; the more linear they are, the smaller the dipole. Panel (c) shows the dipole moment distribution of water as a function of the distance to the oxygen atoms of the nearest $[OAc]^-$ anion in system B: water molecules in direct proximity to an $[OAc]^-$ ion possess higher dipole moments in agreement with Fig. 11. In panel (d), the dependence of the water dipole moment (system D) on the length of the hydrogen bond to another water molecule is represented. When the Ow–Hw distance of the donated hydrogen bond gets smaller (and thus the hydrogen bond gets stronger), the water molecule which is donating the hydrogen bond has in average a higher dipole moment.

3.6 Hydrogen bond geometry

Several authors^{32,33,38,54,56,57,60} investigated the existence of hydrogen bonding in ionic liquids and how they affect their physicochemical properties. The strong ability of the ionic liquid $[C_2C_1Im][OAc]$ to form a hydrogen bond network is reflected by its potentiality to dissolve compounds such as cellulose. A first step towards understanding the solvation process is characterizing the hydrogen bonding network of the solvent.⁵⁷ In Fig. 13, we show a CDF, in which the X axis represents the distance from the hydrogen atom H2 of the $[C_2C_1Im]^+$ cation to an oxygen atom O' of the $[OAc]^-$ anion,

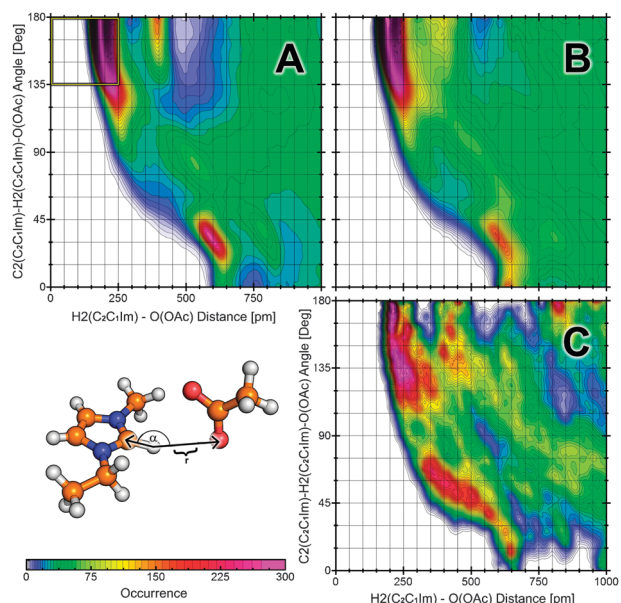


Fig. 13 Combined distribution function showing the hydrogen bond geometry between the atom H2 of the $[C_2C_1Im]^+$ cation and the oxygen atoms of the $[OAc]^-$ anion. The yellow rectangle in plot A indicates the coordination criterion used in Table 5.

and the Y axis depicts the angle defined by the vector which goes from the H2 atom to the C2 atom of the cation and the vector connecting the atom H2 and the oxygen O' of the anion. A value of this angle of 180° indicates that the atoms C2, H2 and O' are aligned (the hydrogen bond would be perfectly linear). A very intense peak in the region around 200 pm/135–180° is present for all three considered systems, related to the hydrogen bond donated from the H2 atom of the $[C_2C_1Im]^+$ cation and accepted for the O' atom of the $[OAc]^-$ anion. A second distinct peak in the region of 600 pm/30° (more intense in the case of the pure ionic liquid and more diffuse when the water content increases) stems from the oxygen atoms of the anion coordinated to H4/H5 atoms of the cation. We see that the hydrogen bond geometry between the cation and anion stays qualitatively the same for the pure liquid and the system with lower water content. The hydrogen bond interactions in the $[C_2C_1Im][OAc]$ are quite strong, as even for small concentrations of IL in water, the cation and anion adopt hydrogen-bond like conformations (strong peak in panel (c) of Fig. 13), even if the distance (see also panel (b) of Fig. 3) and the angle adopted are slightly larger than in the pure liquid.

We will analyze now the hydrogen bond between the $[C_2C_1Im]^+$ cation and water. Fig. 14 presents a CDF, in which the X axis depicts the distance between the atom H2 of the cation and the oxygen atom Ow of water, and the Y axis shows the angle formed between the vectors connecting H2 and C2, and H2 and Ow. The results are essentially similar to those presented for the hydrogen bond between the cation and anion (see Fig. 13). The hydrogen bond network formed by water with the $[C_2C_1Im]^+$ cation is qualitatively similar to that created by the cation and anion, in good agreement with the radial distribution functions presented in Fig. 3. The main difference between the hydrogen bonds present between the cation and anion and those formed between the cation and

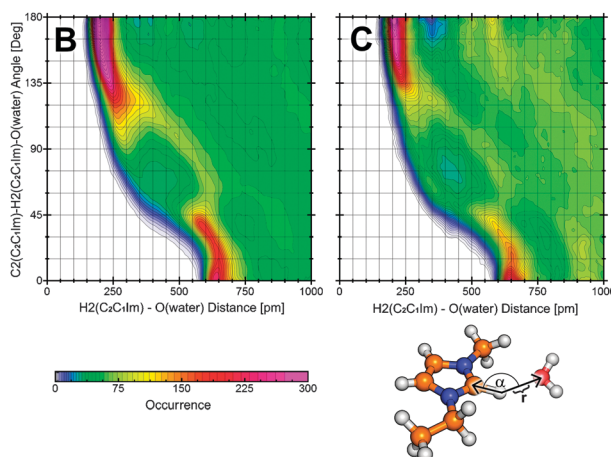


Fig. 14 Combined distribution function showing the hydrogen bond geometry between H2 of the $[C_2C_1Im]^+$ cation and the oxygen atoms Ow of the water molecules.

water (for the system with lower water content) comes from the angular distribution, that is broader in the case of water. For system C (small quantity of IL dissolved in water) when the cation is coordinated to a water molecule, the conformations correspond to a hydrogen bond type arrangement, with a narrower angular distribution, which is shifted towards higher angles when compared with system B.

We define a geometrical coordination criterion that will allow us to clarify and quantify the competition of the acetate anion and the water molecules to coordinate to the most acidic hydrogen atom (H2) of the 1-ethyl-3-methylimidazolium cation. The adopted definition considers that a water molecule or a $[OAc]^-$ anion is coordinated to the atom H2 of the cation if the distance from the oxygen atom to the H2 atom is lower than 250 pm and the angle formed by the atoms C2, H2 and O' ($[OAc]^-$) or Ow (water) is within the range of 135–180° (see yellow rectangle in Fig. 13). Table 5 summarizes the probabilities for one or more water molecules and $[OAc]^-$ anions of being coordinated to a certain H2 atom of a $[C_2C_1Im]^+$ cation. For the pure IL, the 77% of the time the H2 atom is coordinated to a $[OAc]^-$ through a hydrogen bond, whereas for system C (which mainly consists of water) the H2 atom forms an hydrogen bond with a water molecule the 42% of the time, and only the 2% of the time an hydrogen bond with an anion is present. The remaining 55% of the time, the cation adopts conformations where no hydrogen bonds are present at H2. In system B, acetate is found to be bound to the H2 atom of the $[C_2C_1Im]^+$ only slightly more often (35%) than water (29%). Overall, around the 65% of the time, conformations where hydrogen bonding is present at H2 occur. We can conclude that water and the acetate anion compete to

Table 5 Percentage of $[C_2C_1Im]^+$ cations that have at least one water molecule/at least one $[OAc]^-$ anion coordinated to H2. The coordination criterion is represented by the yellow rectangle in Fig. 13

System	H1···O(OAc) [%]	H1···O(water) [%]
A	77.1	
B	35.3	29.4
C	2.3	42.1

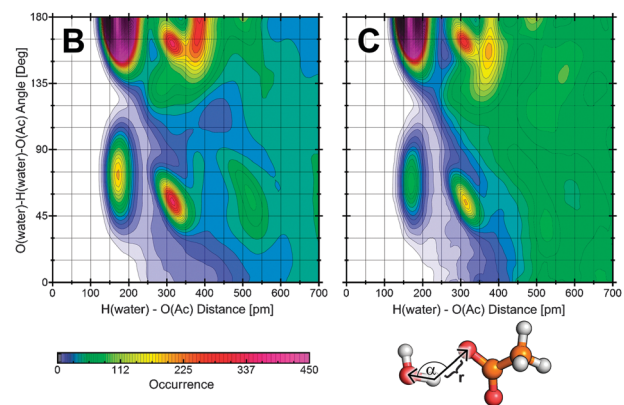


Fig. 15 Combined distribution function showing the hydrogen bond geometry between $[OAc]$ and water.

form hydrogen bonds with the H2 atom of the cation, with the bonding ability of water being lower than that of the anion: less hydrogen bonds are formed between water and the cation, and lower number of hydrogen bond conformations are present when the water content in the system increases, in agreement with the results obtained for different research groups using NMR and IR spectroscopic techniques.^{106–108}

Now we will analyze the hydrogen bond between $[OAc]^-$ and water, which is expected to be very strong. The according CDF, presented in Fig. 15, shows the distance between the oxygen atom O' of $[OAc]^-$ and a hydrogen atom of water on the X axis, and the angle between the vector from H_w to O_w and the vector connecting H_w of a water molecule and O' of a $[OAc]^-$ anion on the Y axis. The strong peak at 175 pm/180° results from the hydrogen bond between H_w and O'. This peak is very intense for both systems B and C, indicating that this hydrogen bond is present almost all the time. The other three peaks in the region from 300 pm to 400 pm result from the fact that a $[OAc]^-$ anion has two oxygen atoms and a water has two hydrogen atoms, so four different entries in the CDF for each pair water– $[OAc]^-$ are present.

To have a complete picture of the hydrogen bond network existent in the systems studied in the present article, we analyze the hydrogen bonding between water molecules. A similar CDF (Fig. 16) to those presented previously is constructed, the X axis represents the distance between an oxygen atom Ow of a water molecule and the hydrogen atom H_w of a different molecule, whereas the Y axis depicts the angle between the vector connecting H_w (water1) to O_w (water1) and the vector from H_w (water1) to O_w (water2). For the system containing pure water (system D) we observe two strong peaks, one centered at distances around 175 pm and angles between 150° and 180° reflecting the well established¹²⁰ strong hydrogen bond between water molecules, whereas the second peak, centered at around 325 pm and angles between 40° and 60° is related to the second hydrogen atom of the water molecule not directly involved in the hydrogen bonding. Insignificant differences are observed when ionic liquid is added to water, the CDFs for systems B and C are similar to that of system D, only a slight broadening of the peaks is remarked: water molecules present in the ionic liquid try to keep their hydrogen bonding network when they are not interacting directly with the cations and anions.

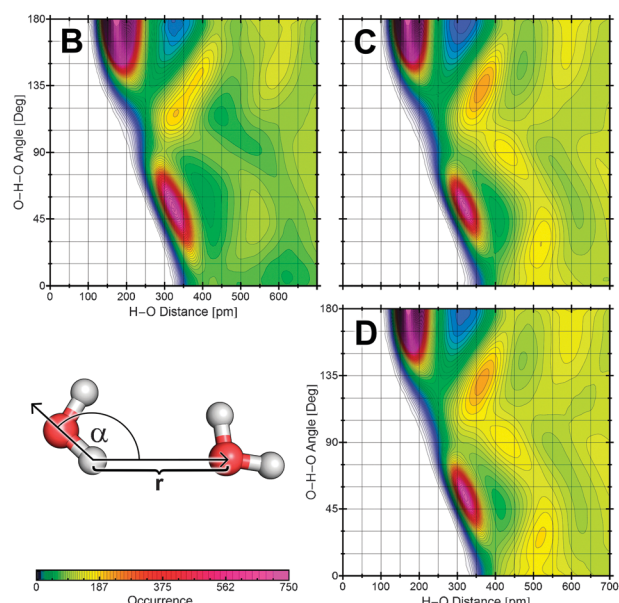


Fig. 16 Combined distribution function showing the hydrogen bond geometry between two water molecules.

4 Conclusion

We presented in this article a comprehensive study on the structure of mixtures of the ionic liquid 1-ethyl-3-methylimidazolium acetate with water using *ab initio* molecular dynamics simulations. Four different systems were considered: pure ionic liquid, pure water, and two binary mixtures, the first with a molar fraction of water $x_{\text{water}} = 0.75$ (24.1% m/m) and the second with $x_{\text{water}} = 0.99$ (91.4% m/m). There is a strong hydrogen bond network present in this ionic liquid, formed between cations, anions and water. The geometry of the hydrogen bonds present in the systems is only slightly dependent on the composition of the systems.

The length of the bonds between the hydrogen and carbon atoms of the imidazolium ring is larger for the pure system, the addition of water leads to a shrink of the bonds. This is related to the strong hydrogen bond ability of the acetate anion that tends to abstract a hydrogen atom of the cation, leading to the formation of carbenes and acetic acid. The geometry of the anion (C^1-C^2 bond length and $\text{O}'-\text{C}^1-\text{O}'$ angle) is also affected. During the length of the simulation there are events where the proton transfer from the imidazolium ring to the acetate anion almost occurs, a fact less probable when the water content increases. Therefore, for the pure $[\text{C}_2\text{C}_1\text{Im}][\text{OAc}]$ the presence of impurities in the form of carbenes is inherent,¹⁰² and the presence of water will make the ionic liquid more stable towards the carbene formation. Water itself does not induce carbene formation, an aspect that can be rationalized in terms of the strength of the hydrogen bonds: acetate forms stronger hydrogen bonds with the imidazolium cation than water. The proton abstraction effect also occurs between water and the acetate anion, there are conformations in the simulations where the water protons are shared between their water molecules and the $[\text{OAc}]^-$ anion, and this effect is independent of the water content. Water in the ionic liquid $[\text{C}_2\text{C}_1\text{Im}][\text{OAc}]$ prevents the formation of carbenes by proton transfer from the cation to the

anion, but not the formation of acetic acid involving water and the anion.

The dipole moment of the $[\text{C}_2\text{C}_1\text{Im}]^+$ cation is unaffected by the water concentration, whereas the dipole moment of the $[\text{OAc}]^-$ anion increases strongly with the water content. On average, water is depolarized by the addition of the ionic liquid, but the dipole moment of a water molecule strongly depends on its local neighborhood. An opposite effect of cations and anions is observed: water molecules in next neighborhood to $[\text{C}_2\text{C}_1\text{Im}]^+$ cations have smaller dipole moments than in average, indicating that water is depolarized^{110,117} by the cation, whereas water molecules in close proximity to $[\text{OAc}]^-$ show strongly increased dipole moments, *i.e.* they get polarized by the acetate.

This is the first of a series of investigations at the microscopic level, with the aid of AIMD, on the ionic liquid 1-ethyl-3-methylimidazolium acetate in interplay with impurities, other (molecular) solvents and different kind of solutes. Although in the present article we dealt only with the pure ionic liquid and its mixtures with water, trying to understand and rationalize the effect of hydrogen bonding, we obtain already many hints for understanding the microscopic characteristics of these systems, also in regards towards the interaction with solutes. In the following articles we will delve deeper into this subject. The use of AIMD, a method that allows us to study condensed phases with an explicit electronic structure calculation, seems to be the recommended tool to explore the hydrogen bond interactions present in the ionic liquids. The intrinsic complexity of ionic liquids, the presence of impurities or dissolved compounds will modify the delicate balance between the different types of interactions. This fact is clear from the present work for the hydrogen bonding interactions, as we show multiple effects of the cation, anion and water on the hydrogen bond network. We are still far from the rationalization of the hydrogen bonding effect on the physico-chemical properties of ionic liquids and a large effort is still necessary.

Acknowledgements

This work was supported by the DFG, in particular by the projects KI-768/5-2 and KI-768/5-3 from the SPP-IL program. The participation of ASP was made possible by a postdoctoral fellowship granted by the DFG through the SPP-IL program. Support from the DFG within the Graduate School of Excellence “Building with Molecules and Nano-objects” (BuildMoNa), the ESF and the IRTG “Diffusion in Porous Materials” is gratefully acknowledged. We would like to thank Jim Davis for helpful discussions.

References

- 1 P. Walden, *Bull. Acad. Imp. Sci. St.-Petersbourg*, 1914, **8**, 405–422.
- 2 A. Maia, *Mini-Rev. Org. Chem.*, 2011, **8**, 178–185.
- 3 G. Stephens and P. Licence, *Chim. Oggi*, 2011, **29**, 72–75.
- 4 T. Welton, *Green Chem.*, 2011, **13**, 225.
- 5 M. J. Earle, J. M. S. S. Esperanca, M. A. Gilea, J. N. Canongia Lopes, L. P. N. Rebelo, J. W. Magee, K. R. Seddon and J. A. Widgren, *Nature*, 2006, **439**, 831–834.

- 6 D. H. Zaitsau, G. J. Kabo, A. A. Strechan, Y. U. Paulechka, A. Tschersich, S. P. Verevkin and A. Heintz, *J. Phys. Chem. A*, 2006, **110**, 7303–7306.
- 7 J. P. Hallett and T. Welton, *Chem. Rev.*, 2011, **111**, 3508–3576.
- 8 I. Krossing, J. M. Slattery, C. Daguenet, P. J. Dyson, A. Oleinikova and H. Weingartner, *J. Am. Chem. Soc.*, 2006, **128**, 13427–13434.
- 9 S. Bouquillon, T. Courant, D. Dean, N. Gathergood, S. Morrissey, B. Pegot, P. J. Scammells and R. D. Singer, *Aust. J. Chem.*, 2007, **60**, 843–847.
- 10 P. S. Schulz, N. Muller, A. Bosmann and P. Wasserscheid, *Angew. Chem., Int. Ed.*, 2007, **46**, 1293–1295.
- 11 P. C. Howlett, D. R. MacFarlane and A. F. Hollenkamp, *Electrochem. Solid-State Lett.*, 2004, **7**, A97–A101.
- 12 E. Markevich, V. Baranchugov and D. Aurbach, *Electrochem. Commun.*, 2006, **8**, 1331–1334.
- 13 J. H. Shin, W. A. Henderson, S. Scaccia, P. P. Prosini and S. Passerini, *J. Power Sources*, 2006, **156**, 560–566.
- 14 Q. Dai, D. B. Menzies, D. R. MacFarlane, S. R. Batten, S. Forsyth, L. Spiccia, Y. B. Cheng and M. Forsyth, *C. R. Chim.*, 2006, **9**, 617–621.
- 15 D. Kuang, P. Wang, S. Ito, S. M. Zakeeruddin and M. Grätzel, *J. Am. Chem. Soc.*, 2006, **128**, 7732–7733.
- 16 T. Oda, S. Tanaka and S. Hayase, *Sol. Energy Mater. Sol. Cells*, 2006, **90**, 2696–2709.
- 17 D. Wei, *Int. J. Mol. Sci.*, 2010, **11**, 1103–1113.
- 18 A. Jimenez and M. Bermudez, *Tribol. Lett.*, 2010, **37**, 431–443.
- 19 M. Palacio and B. Bhushan, *Tribol. Lett.*, 2010, **40**, 247–268.
- 20 A. Podgorsek, G. Salas, P. S. Campbell, C. C. Santini, A. A. H. Pádua, M. F. Costa Gomes, B. Fenet and Y. Chauvin, *J. Phys. Chem. B*, 2011, **115**, 12150–12159.
- 21 P. S. Campbell, C. C. Santini and Y. Chauvin, *Chim. Oggi*, 2010, **28**, 36.
- 22 P. S. Campbell, A. Podgorsek, T. Gutel, C. C. Santini, A. A. H. Pádua, M. F. Costa Gomes, F. Bayard, B. Fenet and Y. Chauvin, *J. Phys. Chem. B*, 2010, **114**, 8156–8165.
- 23 U. L. Bernard, E. I. Izgorodina and D. R. MacFarlane, *J. Phys. Chem. C*, 2010, **114**, 20472–20478.
- 24 P. A. Hunt, I. R. Gould and B. Kirchner, *Aust. J. Chem.*, 2007, **60**, 9–14.
- 25 H. Li, M. Ibrahim, I. Agberemi and M. N. Kobrak, *J. Chem. Phys.*, 2008, **129**, 124507.
- 26 S. Tsuzuki, H. Tokuda, K. Hayamizu and M. Watanabe, *J. Phys. Chem. B*, 2005, **109**, 16474–16481.
- 27 S. Tsuzuki, H. Tokuda and M. Mikami, *Phys. Chem. Chem. Phys.*, 2007, **9**, 4780–4784.
- 28 S. Zahn, F. Uhlig, J. Thar, C. Spickermann and B. Kirchner, *Angew. Chem., Int. Ed.*, 2008, **47**, 3639–3641.
- 29 S. Zahn, G. Bruns, J. Thar and B. Kirchner, *Phys. Chem. Chem. Phys.*, 2008, **10**, 6921–6924.
- 30 E. I. Izgorodina, *Phys. Chem. Chem. Phys.*, 2011, **13**, 4189–4207.
- 31 V. Kempfer and B. Kirchner, *J. Mol. Struct.*, 2010, **972**, 22–34.
- 32 S. B. C. Lehmann, M. Roatsch, M. Schöpke and B. Kirchner, *Phys. Chem. Chem. Phys.*, 2010, **12**, 7473–7486.
- 33 E. I. Izgorodina and D. R. MacFarlane, *J. Phys. Chem. B*, 2011, **115**, 14659–14667.
- 34 M. Goswami and E. Arunan, *Phys. Chem. Chem. Phys.*, 2009, **11**, 8974–8983.
- 35 G. C. Pimentel and A. L. McClellan, *The Hydrogen Bond*, W. H. Freeman and Co., San Francisco, 1960.
- 36 R. L. Gardas, H. F. Costa, M. G. Freire, P. J. Carvalho, I. M. Marrucho, I. M. A. Fonseca, A. G. M. Ferreira and J. A. P. Coutinho, *J. Chem. Eng. Data*, 2008, **53**, 805–811.
- 37 L. G. Sanchez, J. R. Espel, F. Onink, G. W. Meindersma and A. B. de Haan, *J. Chem. Eng. Data*, 2009, **54**, 2803–2812.
- 38 E. W. Castner Jr. and J. F. Wishart, *J. Chem. Phys.*, 2010, **132**, 120901.
- 39 E. M. Siedlecka, M. Czerwcka, S. Stolte and P. Stepnowski, *Curr. Org. Chem.*, 2011, **15**, 1974–1991.
- 40 A. K. A. Sada, A. M. Greenway, P. B. Hitchcock, T. J. Mohammed, K. R. Seddon and J. A. Zora, *J. Chem. Soc., Chem. Commun.*, 1986, 1753–1754.
- 41 D. T. Bowron, C. D'Agostino, L. F. Gladden, C. Hardacre, J. D. Holbrey, M. C. Lagunas, J. McGregor, M. D. Mantle, C. L. Mullan and T. G. A. Youngs, *J. Phys. Chem. B*, 2010, **114**, 7760–7768.
- 42 N. R. Dhumal, H. J. Kim and J. Kiefer, *J. Phys. Chem. A*, 2009, **113**, 10397–10404.
- 43 K. Fumino, T. Peppel, M. Geppert-Rybczynska, D. H. Zaitsau, J. K. Lehmann, S. P. Verevkin, M. Koeckerling and R. Ludwig, *Phys. Chem. Chem. Phys.*, 2011, **13**, 14064–14075.
- 44 K. Fumino, A. Wulf and R. Ludwig, *Phys. Chem. Chem. Phys.*, 2009, **11**, 8790–8794.
- 45 Y. Gao, L. Zhang, Y. Wang and H. Li, *J. Phys. Chem. B*, 2010, **114**, 2828–2833.
- 46 J. Kiefer, K. Obert, A. Boesmann, T. Seeger, P. Wasserscheid and A. Leipertz, *ChemPhysChem*, 2008, **9**, 1317–1322.
- 47 J. Kiefer, K. Obert, S. Himmeler, P. S. Schulz, P. Wasserscheid and A. Leipertz, *ChemPhysChem*, 2008, **9**, 2207–2213.
- 48 K. Noack, P. S. Schulz, N. Paape, J. Kiefer, P. Wasserscheid and A. Leipertz, *Phys. Chem. Chem. Phys.*, 2010, **12**, 14153–14161.
- 49 T. Peppel, C. Roth, K. Fumino, D. Paschek, M. Koeckerling and R. Ludwig, *Angew. Chem., Int. Ed.*, 2011, **50**, 6661–6665.
- 50 C. Roth, T. Peppel, K. Fumino, M. Koeckerling and R. Ludwig, *Angew. Chem., Int. Ed.*, 2010, **49**, 10221–10224.
- 51 J. Stoimenovski, E. I. Izgorodina and D. R. Macfarlane, *Phys. Chem. Chem. Phys.*, 2010, **12**, 10341–10347.
- 52 D. Y. Xing, N. Peng and T. Chung, *J. Membr. Sci.*, 2011, **380**, 87–97.
- 53 T. G. A. Youngs, J. D. Holbrey, C. L. Mullan, S. E. Norman, M. C. Lagunas, C. D'Agostino, M. D. Mantle, L. F. Gladden, D. T. Bowron and C. Hardacre, *Chem. Sci.*, 2011, **2**, 1594–1605.
- 54 A. Wulf, K. Fumino and R. Ludwig, *Angew. Chem., Int. Ed.*, 2010, **49**, 449–453.
- 55 K. Fumino, A. Wulf and R. Ludwig, *Angew. Chem., Int. Ed.*, 2008, **47**, 8731–8734.
- 56 A. Wulf, K. Fumino, D. Michalik and R. Ludwig, *ChemPhysChem*, 2007, **8**, 2265–2269.
- 57 Z. Papanyan, C. Roth, D. Paschek and R. Ludwig, *ChemPhysChem*, 2011, **12**, 2400–2404.
- 58 M. Kohagen, M. Brehm, J. Thar, W. Zhao, F. Müller-Plathe and B. Kirchner, *J. Phys. Chem. B*, 2011, **115**, 693–702.
- 59 P. Bonhôte, A.-P. Dias, N. Papageorgiou, K. Kalyanasundaram and M. Grätzel, *Inorg. Chem.*, 1996, **35**, 1168–1178.
- 60 P. A. Hunt, *J. Phys. Chem. B*, 2007, **111**, 4844–4853.
- 61 T. Endo, T. Kato and K. Nishikawa, *J. Phys. Chem. B*, 2010, **114**, 9201–9208.
- 62 H. Zhao, L. Jackson, Z. Song and O. Olubajo, *Tetrahedron: Asymmetry*, 2006, **17**, 2491–2498.
- 63 H. Du and X. Qian, *Carbohydr. Res.*, 2011, **346**, 1985–1990.
- 64 R. Sescousse, K. A. Le, M. E. Ries and T. Budtova, *J. Phys. Chem. B*, 2010, **114**, 7222–7228.
- 65 A. Brandt, J. P. Hallett, D. J. Leak, R. J. Murphy and T. Welton, *Green Chem.*, 2010, **12**, 672–679.
- 66 Y. Zhang and J. Y. G. Chan, *Energy Environ. Sci.*, 2010, **3**, 408–417.
- 67 S. H. Lee, T. V. Doherty, R. J. Linhardt and J. S. Dordick, *Biotechnol. Bioeng.*, 2009, **102**, 1368–1376.
- 68 N. Sun, M. Rahman, Y. Qin, M. L. Maxim, H. Rodriguez and R. D. Rogers, *Green Chem.*, 2009, **11**, 646–655.
- 69 Y. Qin, X. Lu, N. Sun and R. D. Rogers, *Green Chem.*, 2010, **12**, 968–971.
- 70 M. B. Shiflett and A. Yokozeki, *J. Chem. Eng. Data*, 2009, **54**, 108–114.
- 71 K. R. Seddon, A. Stark and M.-J. Torres, *Pure Appl. Chem.*, 2000, **72**, 2275–2287.
- 72 B. L. Bhargava, Y. Yasaka and M. L. Klein, *Chem. Commun.*, 2011, **47**, 6228–6241.
- 73 H. Liu, K. L. Sale, B. A. Simmons and S. Singh, *J. Phys. Chem. B*, 2011, **115**, 10251–10258.
- 74 C. Krekeler, J. Schmidt, Y. Y. Zhao, B. Qiao, R. Berger, C. Holm and L. Delle Site, *J. Chem. Phys.*, 2008, **129**, 174503.
- 75 J. Schmidt, C. Krekeler, F. Dommert, Y. Y. Zhao, R. Berger, L. Delle Site and C. Holm, *J. Phys. Chem. C*, 2010, **114**, 6150–6155.
- 76 B. L. Bhargava and S. Balasubramanian, *J. Chem. Phys.*, 2005, **123**, 144505.
- 77 B. L. Bhargava, S. Balasubramanian and M. L. Klein, *Chem. Commun.*, 2008, 3339–3351.
- 78 *The PyMOL Molecular Graphics System, Version 1.3*, Schrödinger, LLC, 2010.

- Published on 02 March 2012. Downloaded by East China University of Science & Technology on 4/18/2024 7:24:08 AM.
-
- 79 M. Tarini, P. Cignoni and C. Montani, *IEEE Trans. Visualization Comput. Graphics*, 2006, **12**, 1237–1244.
- 80 H. J. C. Berendsen, D. van der Spoel and R. van Drunen, *Comput. Phys. Commun.*, 1995, **91**, 43–56.
- 81 G. A. Kaminski, R. A. Friesner, J. Tirado-Rives and W. L. Jorgensen, *J. Phys. Chem. B*, 2001, **105**, 6474–6487.
- 82 Z. Liu, S. Huang and W. Wang, *J. Phys. Chem. B*, 2004, **108**, 12978–12989.
- 83 CP2k developers group (GNU General Public License) see: <http://cp2k.berlios.de/index.html>.
- 84 J. VandeVondele, M. Krack, F. Mohamed, M. Parrinello, T. Chassaing and J. Hutter, *Comput. Phys. Commun.*, 2005, **167**, 103–128.
- 85 J. VandeVondele and J. Hutter, *J. Chem. Phys.*, 2003, **118**, 4365–4369.
- 86 P. Hohenberg and W. Kohn, *Phys. Rev. B: Solid State*, 1964, **136**, 864.
- 87 W. Kohn and L. Sham, *Phys. Rev.*, 1965, **140**, 1133.
- 88 A. Becke, *Phys. Rev. A: At., Mol., Opt. Phys.*, 1988, **38**, 3098–3100.
- 89 C. Lee, W. Yang and R. Parr, *Phys. Rev. B: Condens. Matter Mater. Phys.*, 1988, **37**, 785–789.
- 90 S. Grimme, *J. Comput. Chem.*, 2006, **27**, 1787–1799.
- 91 J. VandeVondele and J. Hutter, *J. Chem. Phys.*, 2007, **127**, 114105.
- 92 S. Goedecker, M. Teter and J. Hutter, *Phys. Rev. B: Condens. Matter Mater. Phys.*, 1996, **54**, 1703–1710.
- 93 C. Hartwigsen, S. Goedecker and J. Hutter, *Phys. Rev. B: Condens. Matter Mater. Phys.*, 1998, **58**, 3641–3662.
- 94 S. Nose, *J. Chem. Phys.*, 1984, **81**, 511–519.
- 95 S. Nose, *Mol. Phys.*, 1984, **52**, 255–268.
- 96 G. Martyna, M. L. Klein and M. Tuckerman, *J. Chem. Phys.*, 1992, **97**, 2635–2643.
- 97 G. H. Wannier, *Phys. Rev.*, 1937, **52**, 191–197.
- 98 N. Marzari and D. Vanderbilt, *Phys. Rev. B: Condens. Matter Mater. Phys.*, 1997, **56**, 12847–12865.
- 99 M. Brehm and B. Kirchner, *J. Chem. Inf. Model.*, 2011, **51**(8), 2007–2023.
- 100 Grace, (c) Grace Development Team, 1996–2008, see: <http://plasma-gate.weizmann.ac.il/Grace>.
- 101 Wolfram Research, Inc., *Mathematica*, Version 8.0, Champaign, IL, 2010.
- 102 H. Rodriguez, G. Gurau, J. D. Holbrey and R. D. Rogers, *Chem. Commun.*, 2011, **47**, 3222–3224.
- 103 O. Holloczki, D. Gerhard, K. Massone, L. Szarvas, B. Nemeth, T. Veszpremi and L. Nyulaszi, *New J. Chem.*, 2010, **34**, 3004–3009.
- 104 J. Thar, M. Brehm, A. P. Seitsonen and B. Kirchner, *J. Phys. Chem. B*, 2009, **113**, 15129–15132.
- 105 M. Brüssel, M. Brehm and B. Kirchner, *Phys. Chem. Chem. Phys.*, 2011, **13**, 13617–13620.
- 106 A. Mele, C. D. Tran and S. H. De Paoli Lacerda, *Angew. Chem., Int. Ed.*, 2003, **42**, 4364–4366.
- 107 L. Cammarata, S. G. Kazarian, P. A. Salter and T. Welton, *Phys. Chem. Chem. Phys.*, 2001, **3**, 5192–5200.
- 108 M. Moreno, F. Castiglione, A. Mele, C. Pasqui and G. Raos, *J. Phys. Chem. B*, 2008, **112**, 7826–7836.
- 109 T. Takamuku, Y. Kyoshino, T. Shimomura, S. Kittaka and T. Yamaguchi, *J. Phys. Chem. B*, 2009, **113**, 10817–10824.
- 110 C. Spickermann, J. Thar, S. B. C. Lehmann, S. Zahn, J. Hunger, R. Buchner, P. A. Hunt, T. Welton and B. Kirchner, *J. Chem. Phys.*, 2008, **129**, 104505.
- 111 Z. Kelemen, O. Holloczki, J. Nagy and L. Nyulaszi, *Org. Biomol. Chem.*, 2011, **9**, 5362–5364.
- 112 O. Holloczki, P. Terleczky, D. Szieberth, G. Mourgas, D. Gudat and L. Nyulaszi, *J. Am. Chem. Soc.*, 2011, **133**, 780–789.
- 113 R. W. Alder, P. R. Allen and S. J. Williams, *J. Chem. Soc., Chem. Commun.*, 1995, 1267–1268.
- 114 T. L. Amyes, S. T. Diver, J. P. Richard, F. M. Rivas and K. Toth, *J. Am. Chem. Soc.*, 2004, **126**, 4366–4374.
- 115 K. Wendler, S. Zahn, F. Dommerg, R. Berger, C. Holm, B. Kirchner and L. Delle Site, *J. Chem. Theor. Comput.*, 2011, **7**, 3040–3044.
- 116 R. M. Lynden-Bell, *Phys. Chem. Chem. Phys.*, 2010, **12**, 1733–1740.
- 117 S. Zahn, K. Wendler, L. Delle Site and B. Kirchner, *Phys. Chem. Chem. Phys.*, 2011, **13**, 15083–15093.
- 118 P. L. Silvestrelli and M. Parrinello, *J. Chem. Phys.*, 1999, **111**, 3572–3580.
- 119 B. Kirchner and J. Hutter, *J. Chem. Phys.*, 2004, **121**, 5133.
- 120 H.-S. Lee and M. E. Tuckerman, *J. Chem. Phys.*, 2007, **126**, 164501.